

# Growth, Crystal Structure, and Thermopower of Single Crystals of UNi<sub>1.9</sub>Sn

L. Shlyk,\* J. C. Waerenborgh,† and M. Almeida†

\*B. Verkin Institute for Low Temperature Physics and Engineering, 310164 Kharkov, Ukraine; and †Dept. de Química, Instituto Tecnológico e Nuclear, P-2686-953 Sacavém, Portugal

Received July 16, 1999; in revised form September 10, 1999; accepted September 15, 1999

We have grown single crystals of UNi<sub>1.9(1)</sub>Sn from a semi-levitated melt using the Kyropoulos technique. The crystal structure of UNi<sub>1.9(1)</sub>Sn was determined by single-crystal X-ray diffraction and refined to a residual value of  $R = 0.0336$ . This compound crystallizes in the cubic MnCu<sub>2</sub>Al-type structure with the lattice parameter  $a = 6.4633(4)$  Å. The temperature dependence of the thermoelectric power, different from that observed for UNi<sub>2</sub>Sn polycrystalline material, exhibits no anomalies other than a broad peak near 60 K. The present data suggest a high sensitivity of the physical properties of these intermetallics to the presence of vacancies on transition metal sites. © 2000 Academic Press

**Key Words:** UNi<sub>1.9</sub>Sn; single crystal; X-ray diffraction; thermopower.

## 1. INTRODUCTION

Ternary U–Ni–Sn compounds exhibit very unusual physical properties (1–3). So far several phases have been identified, including UNiSn (two polymorphs), UNi<sub>2</sub>Sn, UNi<sub>4</sub>Sn, and U<sub>3</sub>Ni<sub>3</sub>Sn<sub>4</sub>, and all have been studied in polycrystalline form. Recent magnetic and heat capacity data on U<sub>3</sub>Ni<sub>3</sub>Sn<sub>4</sub> single crystals suggest this material exhibits non-Fermi liquid behavior (4). For the UNiSn (MgAgAs-modified Heusler type) and UNi<sub>2</sub>Sn (MnCu<sub>2</sub>Al Heusler type structure) compounds physical properties gradually change with Ni concentration. With increasing Ni concentration the anti-ferromagnetism of UNiSn disappears and enhanced Pauli paramagnetism is observed for UNi<sub>2</sub>Sn. This agrees with the increase in  $5f-d$  hybridization with Ni doping. Furthermore, intriguing properties are observed in the UNi<sub>2</sub>Sn–UNi<sub>2– $\delta$</sub> Sn compounds with a composition consistent with almost full occupation of the transition element sites. Indeed, steplike shifts in susceptibility and electrical resistivity were observed (3) around  $T = 220$  K in UNi<sub>2</sub>Sn polycrystals, and were related to a symmetry-lowering structural transition. However, the existence of the transformation probably depends on Ni concentration, as is apparent from the different behavior of individual samples (1–3). In this

paper we grew crystals having slightly substoichiometric Ni concentrations, anticipating that they might have interesting properties different from those previously observed on polycrystalline material. We report for the first time the structural characterization and thermopower measurements of UNi<sub>1.9</sub>Sn single crystals.

## 2. PREPARATION AND CRYSTAL STRUCTURE REFINEMENT

The growth of uranium stannides is a rather difficult task due to some disadvantageous properties of these materials, like sensitivity to oxygen, relatively high melting points (usually over 1600°C), and volatility of Sn. In our investigation we have applied the Kyropoulos technique based on the growth of crystals from the top into the melt by means of a cooled seed-crystal holder. Bulk charges for the UNi<sub>1.9</sub>Sn crystal growth were prepared by arc melting the elemental components U, Ni, and Sn, each of at least 99.9% purity, in a 1:1.9:1.6 stoichiometry under purified argon atmosphere. Finally single-crystal samples were grown by slow cooling a semilevitated melt of the resulting bulk material in a cold crucible using an induction furnace. The rate of cooling was approximately 30°C/h between 1600 and 1300°C and 60°C/h between 1300 and 800°C. The solid obtained was about 2.5 cm in diameter, and consisted of many single crystalline grains. Single crystals with dimensions ranging from 0.5 to 2 mm<sup>3</sup> were extracted. The excess of 60% Sn added to the initial bulk charges was estimated after several attempts to grow single crystals. This excess was found to be necessary to compensate for evaporation losses during arc melting as well as during the long single crystal growth procedure.

Several approximately equidimensional single crystals were characterized by X-ray diffraction (XRD) at room temperature. All of them had the same cubic face centered crystal structure. Diffracted X-ray intensities were collected at room temperature on an Enraf Nonius CAD-4

**TABLE 1**  
Crystal Data and Details of Crystal Structure Refinement  
of UN<sub>2- $\delta$</sub> Sn

Chemical formula	UNi <sub>2-<math>\delta</math></sub> Sn ( $\delta \approx 0.14$ )
Formula weight	465.90 g mol <sup>-1</sup>
Crystal system	Cubic, face-centered
Space Group	$Fm\bar{3}m$ (No. 225)
$a_0$ (300 K)	6.4633(4) Å
$V$	270.00(1) Å <sup>3</sup>
$Z$	4
$\mu$ (MoK $\alpha$ )	81.35 mm <sup>-1</sup>
Approximate crystal dimensions	0.3 × 0.5 × 0.3 mm
Radiation, wavelength	MoK $\alpha$ , $\lambda = 0.71069$ Å
Monochromator	Graphite
Temperature	295 K
$2\theta$ range	2°–59°
$\omega$ - $2\theta$ scan	$\Delta\omega = 0.90 + 0.35 \tan \theta$
Data set	$-9 \leq h \leq 9, -9 \leq k \leq 9,$ $0 \leq l \leq 9$
Crystal-to-receiving aperture distance	173 mm
Horizontal, vertical aperture	4 mm, 4 mm
Total data	408
Unique data	35
Observed data ( $F_o \geq 4\sigma(F_o)$ ), $n$	35
Number of refined parameters, $p$	6
Extinction correction	$\chi = 0.009(2)^a$
Final agreement factors	
$R1 = \sum   F_o  -  F_c   / \sum  F_o $	0.0336
$wR2 = [\sum [w(F_o^2 - F_c^2)^2] / \sum [w(F_o^2)^2]]^{1/2}$	0.0703
Goof = $[\sum [w(F_o^2 - F_c^2)^2] / (n - p)]^{1/2}$	1.446

<sup>a</sup>  $F_c$  is multiplied by  $\kappa[1 + 0.001 \times \chi \times F_c^2 \times \lambda^3 / \sin(2\theta)]^{-1/4}$ , where  $\kappa$  is the overall scale factor and  $\chi$  the refined extinction parameter (7).

diffractometer with graphite monochromatized MoK $\alpha$  radiation ( $\lambda = 0.71069$  Å) using an  $\omega$ - $2\theta$  scan mode (Table 1). The unit-cell parameter (Table 1) was obtained by least-squares refinement of the setting angles of 25 reflections with  $11^\circ < 2\theta < 45^\circ$ . The measured intensities were corrected for Lorentz polarization effects (5) and for absorption by an empirical method based on  $\psi$  scans (6). The structure was refined by full-matrix least squares based on the squares of the structure factors  $F^2$  (7). Scattering factors for neutral atoms as well as anomalous dispersion corrections were those defined in SHELXL-93 (7). The single-crystal X-ray diffraction data were analyzed assuming a MnCu<sub>2</sub>Al-type structure, space group  $Fm\bar{3}m$ , first reported for UNi<sub>2</sub>Sn by Takabatake *et al.* [1] based on powder XRD analysis. Besides the scale factor and three isotropic temperature factors, an empirical extinction parameter (7) was also refined. The final  $R$  factor obtained was 0.034 assuming full occupancy of the crystallographic sites. In later stages site occupation factors were allowed to vary but only Ni refined to a value lower than 100%, 93(6)% (Table 2). This would correspond to a stoichiometry of UNi<sub>2- $\delta$</sub> Sn ( $\delta \approx 0.14$ ). Besides the value of the Ni site occupation factor, the low

**TABLE 2**  
Crystal data for UNi<sub>1.9(1)</sub>Sn (MnCu<sub>2</sub>Al-type Structure,  
Heusler Type)<sup>a</sup>

Atom		$x$	$y$	$z$	s.o.f.	$U \times 10^2$ (Å <sup>2</sup> )
U	4a	0	0	0	1.00	0.70(8)
Ni	8c	1/4	1/4	1/4	0.93(6)	0.16(3)
Sn	4b	1/2	1/2	1/2	1.00	0.47(9)

<sup>a</sup> Isotropic temperature factors expressed as  $\exp\{-8\pi^2 U[(\sin(\theta)/\lambda)^2]\}$ .

unit-cell parameter estimated for this crystal, 6.4633(4) Å (Table 1), as compared with the value reported in Ref. (1), 6.485 Å, argues in favor of a defect structure. The interatomic distances and coordination numbers are listed in Table 3.

### 3. THERMOPOWER MEASUREMENTS

The thermopower measurements were performed on a single crystal of approximate dimensions  $1 \times 1 \times 2$  mm, previously oriented on the CAD-4 diffractometer. Each end of the sample was fixed on a quartz heat sink in such a way that the temperature gradient was applied along the  $c$  axis (the longest dimension of the crystal). Gold wires were glued to the crystal with silver paste. The temperature difference between the heat sinks as well as the temperature of the sample was measured with Au/chromel thermocouples. The thermopower was finally measured relative to gold by a slow ac technique in an apparatus similar to that described by Chaikin and Kwak (8), with a thermal gradient of 1 K.

**TABLE 3**  
Interatomic distances ( $d$ ) up to 5 Å, and Average Numbers ( $N$ )  
of Nearest Neighbors of U, Ni, and Sn Atoms in Nonequivalent  
Positions in UNi<sub>1.9 $\delta$ (1)</sub>Sn

	$N$	Atoms	$d$ (Å)
U(4a)	7.6	Ni	2.799
	6	Sn	3.232
	12	U	4.570
Sn(4b)	7.6	Ni	2.799
	6	U	3.232
	12	Sn	4.570
Ni(8c)	4	Sn	2.799
	4	U	2.799
	5.7	Ni	3.232
	11.4	Ni	4.570

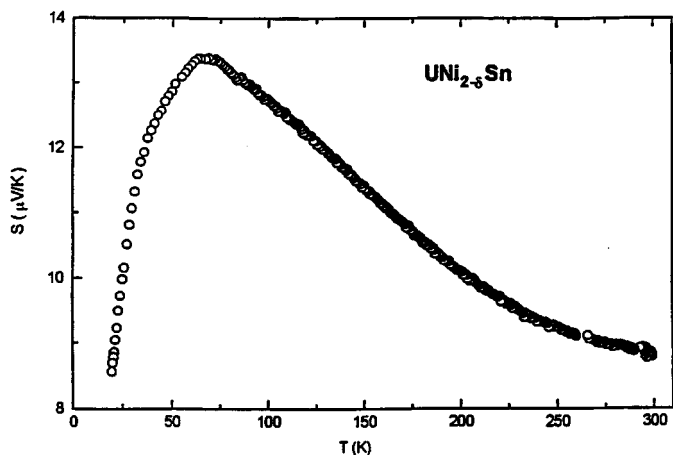


FIG. 1. Temperature dependence of the thermoelectric power of  $\text{UNi}_{2-\delta}\text{Sn}$  ( $\delta \approx 0.14$ ) single crystals.

Measurements in the temperature range 16–300 K (Fig. 1) are significantly different from those reported in Ref. (1) for polycrystalline  $\text{UNi}_2\text{Sn}$ . Starting with a value of  $8.7 \mu\text{V/K}$  at 300 K the thermopower of  $\text{UNi}_{1.9}\text{Sn}$  single crystals increases, reaching a maximum of  $13.5 \mu\text{V/K}$  at around 60 K. In the temperature range 16–60 K the thermopower decreases rapidly to  $8.2 \mu\text{V/K}$  at  $T = 16$  K and follows approximately a  $1/T$  dependence between 50 and 16 K. For the polycrystalline  $\text{UNi}_2\text{Sn}$  material the sign of the thermopower is also positive, but the  $S(T)$  curve tends asymptotically to zero as  $T \rightarrow 0$  K (1).

As follows from Mott's equation for thermopower,

$$S = (-\pi^2 k^2 T / 3 |e|) (\partial \ln N(E) / \partial E + \partial \ln \tau(E) / \partial E), \quad [1]$$

[where  $N(E)$  is the density of states and  $\tau$  is the relaxation time of the conduction electrons] the energy dependence of  $N(E)$  affects significantly the magnitude of the thermopower, assuming that the first term of Eq. [1] is dominant. This assumption means that the second term which is related to the mean free path of the conduction electrons (9) gives a significant contribution at lower temperatures and does not change much particularly in the temperature range in which our data were obtained (16–300 K). This assumption is in agreement with that used to explain the thermopower behavior of other rare-earth compounds (10, 11). Furthermore, the thermopower behavior of some rare-earth compounds, for instance  $R_3\text{Co}$  (where  $R = \text{rare earth}$ ), has been explained on the basis of the  $3d$  band position relative to the Fermi level (11). Similar effects may be expected to affect the thermopower behavior of  $\text{UNi}_{1.9}\text{Sn}$ . In  $\text{UNi}_{1.9}\text{Sn}$  the shift of the Fermi level relative to the band structure as the number of  $3d$  Ni electrons is varied may have a significant effect on thermopower. Yet, considering the U–Ni in-

teratomic distances (see Table 3) a significant  $5f$ – $3d$  hybridization is expected. Hence, the small variation in Ni concentration in  $\text{UNi}_{1.9}\text{Sn}$  relative to  $\text{UNi}_2\text{Sn}$  may play an important role in  $5f$ – $3d$  hybridization which would be reflected in a different shape of the density of states at the Fermi energy. This tentative interpretation of the observed temperature behavior of the thermopower may be confirmed only when data on all transport properties of this new crystal are available. These measurements are now in progress.

#### 4. CONCLUDING REMARKS

The present data provide no evidence for a structural transition below room temperature and, when compared with previous results reported for  $\text{UNi}_2\text{Sn}$  (1–3), suggest that there is a high sensitivity of the physical properties of Heusler-type materials to the presence of vacancies on transition metal sites. Indeed, preliminary measurements of the magnetic properties of  $\text{UNi}_{1.9}\text{Sn}$  single crystals (12) show a behavior different from that observed for polycrystalline material. Detailed magnetic and transport measurements are now underway, to investigate the influence of vacancies on transition metal sites on the physical properties of Heusler-type materials.

#### ACKNOWLEDGMENT

The single-crystal samples were grown by L.S. during her stay in Portugal under the support of a NATO fellowship.

#### REFERENCES

1. T. Takabatake, H. Fujii, S. Miyata, H. Kawanaka, Y. Aoki, T. Suzuki, T. Fujita, Y. Yamaguchi, and J. Sakurai, *J. Phys. Soc. Jpn.* **59**, L16 (1990).
2. F. M. Mulder, A. Drost, R. C. Thiel, and E. Frikkee, *Phys. Rev. Lett* **77**, 3477 (1996).
3. T. Endstra, S. A. M. Mentink, G. J. Nieuwenhuys, J. A. Mydosh, and K. H. J. Bushow, *J. Phys. C: Cond. Matter* **2**, 2447 (1990).
4. L. Shlyk, J. C. Waerenborgh, P. Estrela, L. E. DeLong, A. DeVisser, and M. Almeida, *J. Phys. C* **11**, 3525 (1999).
5. C. K. Fair, MOLEN, Enraf-Nonius, Delft, 1990.
6. A. C. T. North, D. C. Phillips, and F. S. Mathews, *Acta Crystallogr. Sect. A* **24**, 351 (1968).
7. M. Sheldrick, University of Göttingen, Germany, SHELXL-93: Program for Crystal Structure Refinement, 1993.
8. P. M. Chaikin and J. F. Kwak, *Rev. Sci. Instrum.* **46**, 218 (1975).
9. J. M. Ziman, "Electrons and Phonons," p. 397. Univ. Press, Oxford, 1979.
10. K. Yagasaki, T. Burkov, and E. Gratz, *Physica B* **186/88**, 643 (1993).
11. I. Umehara, T. Kuwai, J. Sakurai, K. Maezawa, Q. F. Lu, and K. Sato, *Physica B* **206/207**, 405 (1995).
12. L. Shlyk *et al.*, to be published.